

Deterministic switching of Bloch chirality in magnetic skyrmions: the Dzyaloshinskii astroid

Michael D. Kitcher,^{1,*} Marc De Graef,¹ and Vincent Sokalski¹

¹*Department of Materials Science & Engineering,
Carnegie Mellon University, Pittsburgh, PA 15213, USA*

We present a mechanism for deterministic control of the Bloch chirality in magnetic skyrmions originating from the interplay between an interfacial Dzyaloshinskii–Moriya interaction (DMI) and a perpendicular magnetic field. Although conventional interfacial DMI favors chiral Néel skyrmions, it does not break the energetic symmetry of the two Bloch chiralities in mixed Bloch–Néel skyrmions. However, the energy barrier to switching between Bloch chiralities does depend on the sense of rotation, which is dictated by the direction of the driving field. Our analysis of steady-state Dzyaloshinskii domain wall dynamics culminates in a switching diagram akin to the Stoner–Wohlfarth astroid, revealing the existence of both monochiral and multichiral Bloch regimes. Furthermore, we discuss recent theory of vertical Bloch line–mediated Bloch chirality selection in the precessional regime and extend these arguments to lower driving fields. This work establishes that applied magnetic fields can be used to dynamically switch between the chiral Bloch states of domain walls and skyrmions as indicated by this new *Dzyaloshinskii astroid*.

The internal structure of magnetic skyrmions and domain walls (DWs) is central to the blooming field of chiral magnetism [1]. The origin of this preferred chirality is the Dzyaloshinskii–Moriya interaction (DMI) [2, 3], which can favor chiral Néel DWs in conventional ferromagnet/heavy metal (FM/HM) thin films with structural inversion asymmetry [4, 5], as well as chiral Bloch DWs in B20 magnets which possess bulk inversion asymmetry [6, 7]. Surprisingly, there have been relatively few reported studies of switching between chiral states, which could enable new binary magnetic memory schemes. These efforts have focused on the direct control of the strength and sign of interfacial DMI in FM/HM films via an applied electric field, so as to reverse the Néel chirality of skyrmions [8–10]. However, the desired switched states would remain only if the electric field is applied perpetually.

In this work, we consider switching between the Bloch states of DWs and skyrmions in FM/HM films with perpendicular magnetic anisotropy (PMA) and a conventional interfacial DMI, where the latter preferentially stabilizes one Néel handedness over the other but creates no difference in energy between the two Bloch chiralities. The switching process is driven by an effective out-of-plane magnetic field which causes a reorientation of the internal magnetization of a DW or skyrmion to a steady-state configuration. The pinning-free dynamics of field-driven DWs were first formalized and investigated by Walker, Slonczewski, and Schryer in a series of seminal papers [11–13]. Without DMI, field-based switching was only expected beyond the critical Walker field where a DW undergoes Walker breakdown: the in-plane magnetization of the wall cycles continuously through Bloch states, concurrent with a reduction in the DW’s velocity. Here, we show that for films with interfacial DMI, a range of effective field strengths exist in the steady-state regime where the driving torque enables unidirectional

switching of DWs from one Bloch chirality to another. This chirality remains after the effective field is removed and the system returns to static equilibrium.

The analyses in this work are built upon the following 1D approximations for magnetic domain wall energy, which includes the resting Bloch wall energy (σ_0), domain wall anisotropy energy, and DMI energy [4, 14]:

$$\sigma = \sigma_0 + 2K_d\lambda_0 \cos^2\phi - \pi D \cos\phi; \quad (1a)$$

$$\lim_{t_f \rightarrow 0} K_d = \frac{\ln[2]t_f\mu_0 M_s^2}{2\pi\lambda_0}; \quad (1b)$$

where D is the DMI constant, K_d is the domain wall anisotropy, t_f is the film’s, M_s is the saturation magnetization, $\lambda_0 = \sqrt{A/K_{eff}}$ is the width of the DW, A is the exchange stiffness, K_{eff} is the effective PMA, μ_0 is the vacuum permeability, and ϕ is the in-plane angle between the moment and normal of the DW. (See Figure 1b.) As noted in Figure 1a, a positive DMI constant stabilizes DW moments that point towards a $-M_z$ domain, i.e., a right-handed (RH) Néel DW. Conversely, $D < 0$ favors a left-handed (LH) Néel DW. The clockwise (CW) and counterclockwise (CCW) Bloch windings are likewise defined with respect to a $-M_z$ domain.

It is well known that when $|D| \geq D_c$, where $D_c = \frac{4\lambda_0 K_d}{\pi}$, the DW takes on a fully Néel configuration. In our analyses, we are focused on the regime where $|D| < D_c$ and the DW assumes a mixed Bloch–Néel configuration; the Néel component of the wall has a preferred chirality, whereas both winding directions are equally favored for its Bloch component. The corresponding existence of two energy minima is captured by (1a), as illustrated in Figure 1a. (For clarity, the ϕ -independent contribution of the intrinsic Bloch energy is not included in the plots.) The static equilibrium in-plane magnetization of a DW, obtained when $\sigma_\phi = 0$ and $\sigma_{\phi\phi} > 0$ (subscripts of

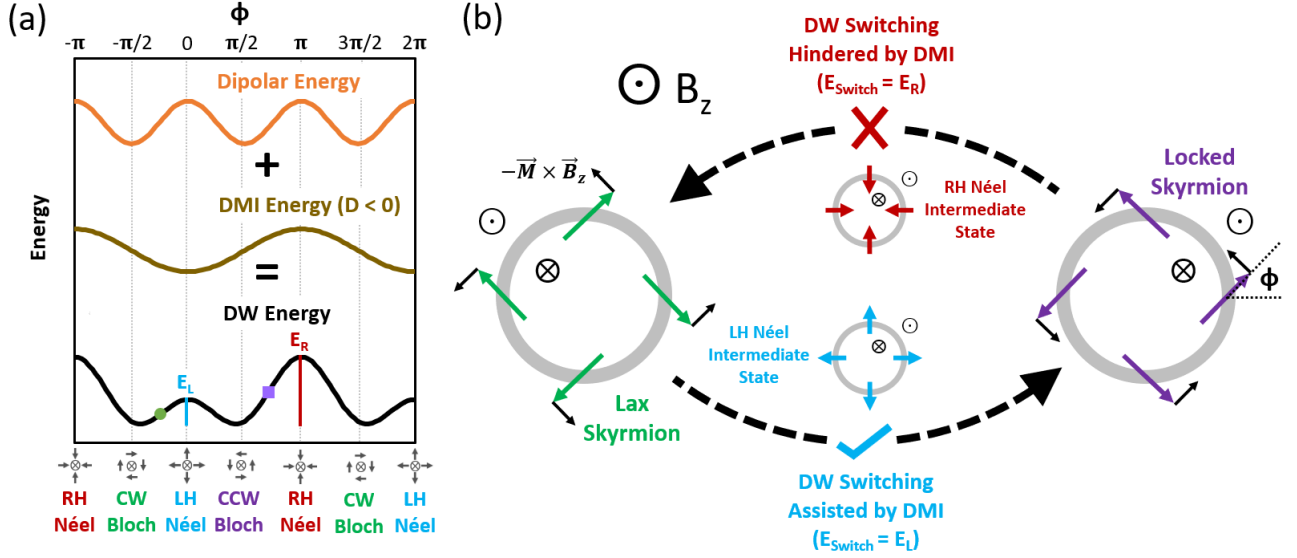


FIG. 1: (a) Plots of the dipolar energy, DMI energy, and total energy versus ϕ for a Dzyaloshinskii DW where $D < 0$. E_L and E_R are the energy barriers to switching between the two Bloch chiralities. For $B_z > 0$, the lability points of the lax and locked walls are labeled with round (green) and square (purple) markers, respectively. (b) Illustration of unidirectional switching between mixed skyrmions for $0 < |D| < D_c$ and $B_{SW} < B < B_W$. For $D < 0$ and $B_z > 0$, DMI promotes the reorientation of a skyrmion with CW Bloch chirality (green moments; the laxed configuration) to one with a CCW Bloch chirality (purple moments; the locked configuration) via the preferred Néel chirality; a transition back to the lax wall, however, is blocked.

σ denote partial derivatives), is then

$$\begin{aligned} \cos \phi &= m_{NG} = \frac{D}{D_c}, & |D| \leq D_c; \\ &= \text{sign}[D], & |D| \geq D_c; \end{aligned} \quad (2a)$$

$$\sin \phi = m_{BG} = \pm \sqrt{1 - (m_{NG})^2}, \quad (2b)$$

where m_{NG} and m_{BG} are the respective Néel and Bloch components of the unit in-plane moment of a DW at static equilibrium (i.e., in its ground state). As such, m_{NG} also equals the relative strength of DMI with respect to the DW anisotropy energy.

We now turn our attention to the dynamic response of DWs subject to an effective perpendicular field. Derived from the Landau–Lifshitz–Gilbert (LLG) equation, the Slonczewski equations of motion for the velocity and internal magnetization of DWs [12, 15] are:

$$\dot{\phi} = \frac{\gamma}{1 + \alpha^2} (-\alpha\Omega + B_z); \quad (3a)$$

$$\dot{q} = \frac{\gamma\lambda_0}{1 + \alpha^2} (\Omega + \alpha B_z); \quad (3b)$$

$$\Omega = \frac{\sigma_\phi}{2\lambda_0 M_s}, \quad (3c)$$

where q is the position of the DW, γ is the gyromagnetic ratio, α is the Gilbert damping constant, B_z is the normalized driving torque, and $-\alpha\Omega$ represents the restoring torque that emerges as moments are driven away from static equilibrium by some $\Delta\phi$.

The steady-state configuration is therefore achieved when these two forces are balanced. From (1a), the normalized restoring torque, σ_ϕ , emerges as

$$\sigma_\phi = -4K_d\lambda_0 \sin \phi \cos \phi + \pi D \sin \phi. \quad (4)$$

At steady state, rearranging (3a) yields

$$\sigma_\phi = \frac{2\lambda_0 B_z M_s}{\alpha}. \quad (5)$$

We can further describe the dynamic response of a DW to a driving field by introducing the concept of *domain wall susceptibility* (χ_{dw}):

$$\chi_{dw} = \left(\frac{\partial B_z}{\partial \phi} \right)^{-1}. \quad (6)$$

Combining (5) and (6) at steady state,

$$\chi_{dw} \propto \sigma_\phi^{-1}, \quad (7)$$

where the proportionality constant is $\frac{2\lambda_0 M_s}{\alpha}$ and σ_ϕ is the corresponding rate of change of the scaled restoring torque with respect to ϕ .

In the absence of DMI, there are two stable DW configurations in the steady-state regime with opposite Bloch chiralities, stemming from the corresponding degeneracy of the two static wall variants. (See the top plot

of Figure 1a.) At a critical B_z —conventionally termed the Walker field—both DWs experience the maximum restoring torque and $|\Delta\phi|$ possible at steady state, being stabilized at equivalent inflection points in the energy landscape (i.e., where $\chi_{dw} \rightarrow \infty$ and the moments of the DW are *labile*, or most inclined to rotate). For B_z values infinitesimally higher than this *lability field*, the restoring torques cannot completely match the driving torque and both walls enter a precessional regime where their in-plane magnetizations rotate continuously. This behavior is accompanied by a sudden drop in the time-averaged velocity of each DW, as revealed in studies of domain expansion [16].

Turning to the case of moderate interfacial DMI ($0 < |D| < D_c$; see Figure 1a), a third possibility emerges: a single steady-state solution which adopts only one Bloch chirality. Although the two Bloch chiralities remain degenerate at static equilibrium, the energetic equivalence of the two Néel chiralities is broken. Beyond a shift in the energy minima towards the favored Néel chirality at static equilibrium, the presence of DMI also manifests as an asymmetry in the energy maxima which correspond to Néel configurations and act as barriers to switching between the two ground states. On account of DMI, the two walls will therefore experience different net restoring torques when driven away from static equilibrium by the same effective field, leading to disparate variations in χ_{dw} during the process. As depicted in Figure 1b, the wall that is driven towards the DMI-preferred Néel configuration—which we term the *lax wall*—experiences an assistive torque from DMI, whereas the driving torque on its counterpart—the *locked wall*—is opposed by the same effective torque generated by DMI. Consequently, the lability field is chirality dependent: the lax wall has the lower critical B_z and larger $\Delta\phi$ at its lability point; Figure 1a illustrates the case of $B_z < 0$. For driving fields in between these two limiting values, this wall will therefore adopt the steady-state configuration—and the Bloch chirality—of the locked wall. We can then characterize the lability field of the lax wall as the DW switching field (B_{SW}), while that of the locked wall remains the Walker field (B_W). From this treatment, it is evident that a single Bloch chirality could be favored in magnetic systems with PMA and interfacial DMI when an effective B_z is present.

Within the framework of the 1D domain wall energy model and the first Slonczewski equation—captured in (1a) and (3a), respectively—we then determine how B_{SW} and B_W depend on DMI. Using the steady-state restoring torque in (5) and the lability condition $\sigma_{\phi\phi} = 0$, the normalized Néel and Bloch wall moments at these lability

points (m_{NL} and m_{BL} , correspondingly) are given by

$$m_{NL} = \cos\phi = \frac{m_{NG} \pm \sqrt{(m_{NG})^2 + 8}}{4}; \quad (8a)$$

$$m_{BL} = \sin\phi = \mp\sqrt{(m_{NL} - m_{NG})m_{NL}} \\ = \mp\sqrt{1 - (m_{NL})^2}. \quad (8b)$$

Here and henceforth, upper and lower signs correspond to expressions for lax and locked walls, respectively, for $D > 0$ (and vice versa for $D < 0$). We note that the locked wall case of (8a) is equal to the expression in [4] for $\cos\phi$ at B_W . Combining these equations with (4), we obtain the critical ratio of driving field to Gilbert damping needed to drive each wall to a labile state:

$$\frac{B_z}{\alpha} = \text{sgn}[B_z] \frac{2K_d}{M_s} (m_{NG} - m_{NL})m_{BL} \\ = \text{sgn}[B_z] \frac{K_d}{8M_s} \sqrt{\pm m_{NG} + \sqrt{(m_{NG})^2 + 8}} \\ \times \sqrt{(\mp 3m_{NG} + \sqrt{(m_{NG})^2 + 8})^3}. \quad (9)$$

The results of this analysis are presented in the form of a DW phase diagram that indicates the critical field required to stabilize a single Bloch chirality for a given DMI strength. By normalizing (9) by $\frac{K_d}{8M_s}$ to obtain the reduced quantity $\frac{b_z}{\alpha}$ and plotting the result as a function of m_{NG} (which is also the reduced DMI), we obtain pairs of lability lines that delineate the various chirality regimes. For the case of $D = 0$, the system directly transitions from the achiral Bloch regime to the precessional regime. As the strength of DMI increases, a window emerges where there is a single steady-state solution (i.e., only one sense of switching is possible) before transitioning to the precessional regime. The monochirality region bears a striking resemblance to the Stoner–Wohlfarth astroid for single-domain switching first proposed by Slonczewski [17, Ch. 3]. As the astroid in Figure 2 characterizes the field-induced switching behavior of Dzyaloshinskii DWs, we propose to term it the *Dzyaloshinskii astroid*. In contrast to the referenced model of single-domain switching, the lability lines retain their physical relevance beyond the switching astroid, becoming the bounds of the precessional regime. As observed in [4], the Bloch component, m_{BG} , of the DW moments at static equilibrium is dominant for DMI values as high as $D = 0.7D_c$, which also lends the Dzyaloshinskii astroid to probing via Lorentz transmission electron microscopy.

Since the Bloch chirality of Dzyaloshinskii DWs at steady state would be preserved after the driving field is removed, these findings pave a promising path towards a non-volatile magnetic memory scheme where information is stored as the Bloch chirality of mixed skyrmions in FM/HM films. Indeed, such a scheme was first presented in 1974 by Slonczewski where carefully timed field pulses

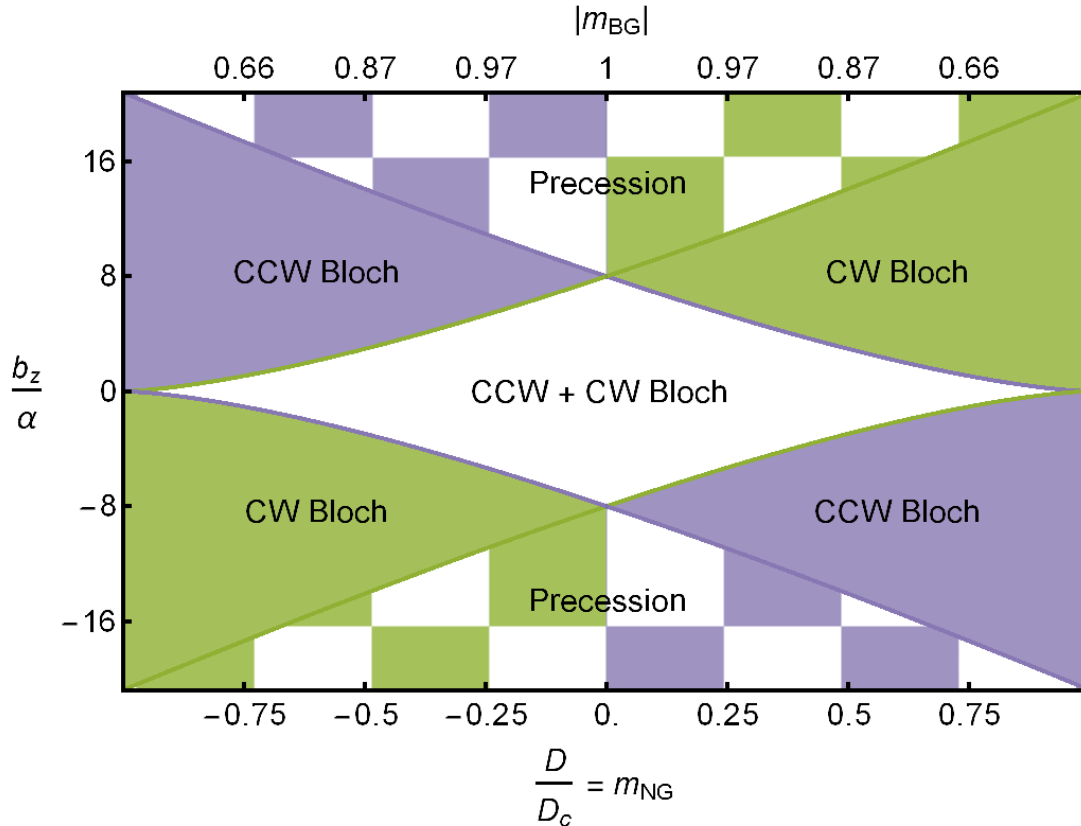


FIG. 2: The Dzyaloshinskii astroid depicting the multichiral Bloch (white), monochiral Bloch (green or purple), and precessional (chequered) regimes for Dzyaloshinskii DWs and mixed skyrmions as a function of reduced DMI and reduced driving field (m_{NG} and $\frac{b_z}{\alpha}$, respectively). Corresponding values of m_{BG} , the normalized Bloch component of magnetization, are also indicated. The various phase boundaries are given by the lability lines for the unidirectional switching field (B_{SW}) and the Walker field (B_W).

in the precessional regime could switch the chirality of Bloch bubbles hosted by iron–garnet films without any reported DMI [18]. The key distinguishing feature of our work is that the Bloch chirality of skyrmions could be written using field pulses in the DMI-induced monochirality regimes, thereby preventing back-switching. The above analysis makes a number of reasonable yet noteworthy assumptions about DW switching—in particular, that the process occurs coherently without the formation of vertical or horizontal Bloch lines (VBLs and HBLs, respectively). Li et al. found that the presence of VBLs increased with decreasing thickness [19, 20]. Moreover, the study in [18] concluded that HBLs mediated switching in the thick films studied; these results have recently been corroborated [21]. These DW substructures would distort the shape of the astroid shown in Figure 2, much like the formation of domains impacts the switching fields given by the Stoner–Wohlfarth astroid. As such, we support the investigation of these mechanisms using micro-

magnetic simulation tools.

Interestingly, recent research indicates that Bloch lines could facilitate Bloch chirality preferences through their interaction with the interfacial DMI field in magnetic thin films. In light of our analysis, the studies presented in [22, 23] suggest that the monochirality regime can extend past the Walker field due to DMI-induced asymmetries in the B_z -dictated nucleation and propagation of the VBLs that mediate DW precession. As theorized in [22], VBLs whose Néel components align with the DMI field have lower energies, larger widths and faster propagation speeds than VBLs of the opposite Néel handedness. Thus, for sufficiently long DWs, the faster VBLs catch up to the slower ones, ultimately preserving the locked wall configuration and its Bloch chirality. We also assert that the preference for VBL evolution that is jointly assisted by B_z and DMI would persist at lower fields, permitting VBL-mediated Bloch chirality asymmetries and an extension of the monochirality regime below the B_{SW}

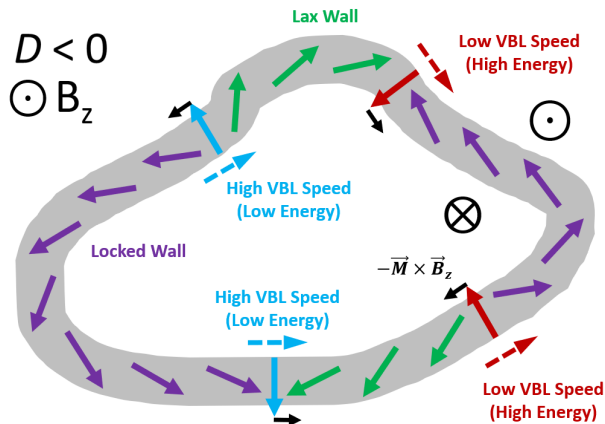


FIG. 3: Illustration of an emergent preference for locked walls (purple)—and their Bloch chirality—when VBL nucleation and propagation are jointly assisted by DMI and B_z . DMI-stabilized VBLs would nucleate preferentially from lax walls (green) and truncate them. Moreover, DMI-favored VBLs have lower energies and higher field-driven velocities than their counterparts, disproportionately increasing the length of locked walls.

values indicated by the Dzyaloshinskii astroid. Given an effective B_z and a driving force for VBL formation, DMI-favored VBLs will nucleate preferentially from the lax wall, move faster than the high-energy VBLs, and are more likely to unwind than their counterparts, yielding in each case a preference for the locked wall and its Bloch chirality. An example of such a scenario is illustrated in Figure 3. This behavior is also in line with observed transitions from π - to 2π -VBLs in multilayer films with $D < D_c$ as the film thickness decreases [19, 20]. Moreover, we anticipate that horizontal Bloch lines would exhibit similarly asymmetric behavior.

Further examining existing literature, we propose that the phenomena theorized above could contribute to the preferred Bloch chiralities observed in asymmetric Fe/Gd- and Co/Pd-based multilayers with an established or expected interfacial DMI [24–27]. Importantly, these observations were made after various out-of-plane field treatments and in the presence of a non-zero B_z . While the authors of [27] attributed these findings to an interlayer DMI, the strength of this interaction and the required microscopic origins were not investigated. Superficially, one would not expect gradually applied magnetic fields (as done in these and other studies) to drive the DWs away from static equilibrium as the films quickly adopt stationary magnetic textures. Recent work, however, suggests that a millisecond-scale B_z pulse in the creep regime can still drive a DW to a steady-state configuration [28]; the effective field, despite its relatively low magnitude, would then be significant during the thermally activated motion of

DWs between pinning sites. Likewise, changes in the effective field could temporarily induce steady-state profiles of DWs during the transient expansion or contraction of domains—and for the appropriate ΔB_z values, unidirectionally switching the Bloch chirality of DWs in the process. Finally, an additional study of one film from [27] that exhibited a Bloch chirality preference uncovered a prevalence of VBLs, determined that VBLs interact via stray fields to stabilize pairs of DWs with opposite Bloch chiralities, and concluded that further studies of their evolution were crucial to understanding Bloch chirality trends in multilayer films [29]. Thus, these results lend credence to our theory of VBL-mediated Bloch chirality preferences in the low- B_z regime.

In conclusion, we have demonstrated that for DWs driven by out-of-plane fields in interfacial DMI systems, the degeneracy between the two possible Bloch windings is broken at steady state due to DMI-induced asymmetries in the restoring torque experienced by the two wall variants. Consequently, a new steady-state regime emerges where DWs of only one Bloch chirality are stabilized as determined by the signs of D and B_z . Using the Slonczewski equations of motion and the 1D domain wall energy model, we derived an effective phase diagram for field-driven Dzyaloshinskii DW switching, which we term the Dzyaloshinskii astroid. Recasting recent studies in the context of our work further revealed that the evolution of vertical Bloch lines—and, more generally, DW substructures—in the presence of interfacial DMI and an effective B_z could extend the bounds of the Bloch monochirality regime beyond the critical lability fields predicted by our 1D analysis. Beyond shedding light on recent reports of Bloch chirality preferences in interfacial DMI systems, these findings present favorable prospects for new non-volatile computing technologies based on the deterministic, writable Bloch chirality of mixed skyrmions and Dzyaloshinskii DWs.

All authors acknowledge the support of the Defense Advanced Research Agency (DARPA) program on Topological Excitations in Electronics (TEE; grant no. D18AP00011), as well as the use of the Materials Characterization Facility at Carnegie Mellon University supported by the grant MCF-677785. M.D.K. is also grateful for the support of the National GEM Consortium, as well as the support of the Neil and Jo Bushnell Engineering Fellowship awarded by Carnegie Mellon University’s College of Engineering.

* mkitcher@andrew.cmu.edu

[1] C. Back, V. Cros, H. Ebert, K. Everschor-Sitte, A. Fert, M. Garst, T. Ma, S. Mankovsky, T. L. Monchesky,

- M. Mostovoy, N. Nagaosa, S. S. Parkin, C. Pfleiderer, N. Reyren, A. Rosch, Y. Taguchi, Y. Tokura, K. V. Bergmann, and J. Zang, *J. Phys. D: Appl. Phys.* **53**, 363001 (2020).
- [2] I. Dzyaloshinsky, *J. Phys. Chem. Solids* **4**, 241 (1958).
- [3] T. Moriya, *Phys. Rev.* **120**, 91 (1960).
- [4] A. Thiaville, S. Rohart, E. Jue, V. Cros, and A. Fert, *EPL* **100**, 57002 (2012).
- [5] A. Hrabec, N. A. Porter, A. Wells, M. J. Benitez, G. Burnell, S. McVitie, D. McGrouther, T. A. Moore, and C. H. Marrows, *Phys. Rev. B* **90**, 10.1103/PhysRevB.90.020402 (2014).
- [6] S. Mühlbauer, B. Binz, F. Jonietz, C. Pfleiderer, A. Rosch, A. Neubauer, R. Georgii, and P. Böni, *Science*, 915 (2009).
- [7] N. Nagaosa and Y. Tokura, *Nat. Nanotechnol.* **8**, 899 (2013).
- [8] K. Nawaoka, S. Miwa, Y. Shiota, N. Mizuochi, and Y. Suzuki, *Appl. Phys. Express* **8**, 063004 (2015).
- [9] T. Srivastava, M. Schott, R. Juge, V. Křížáková, M. Belmeguenai, Y. Roussigné, A. Bernard-Mantel, L. Ranno, S. Pizzini, S.-M. Chérif, A. Stashkevich, S. Auffret, O. Boulle, G. Gaudin, M. Chshiev, C. Baraduc, and H. Béa, *Nano Lett.* **18**, 4871 (2018).
- [10] M. Schott, L. Ranno, H. Béa, C. Baraduc, S. Auffret, and A. Bernard-Mantel, *J. Magn. Magn. Mater.* **520**, 167122 (2021).
- [11] J. Dillon, in *Spin Arrangements and Crystal Structure, Domains, and Micromagnetics*, edited by G. T. Rado and H. Suhl (Academic Press, 1963) pp. 415–464.
- [12] J. Slonczewski, in *AIP Conference Proceedings*, Vol. 5, edited by C. D. Graham and J. J. Rhyne (AIP Publishing, Chicago, 1972) pp. 170–174.
- [13] N. L. Schryer and L. R. Walker, *J. Appl. Phys.* **45**, 5406 (1974).
- [14] J. P. Pellegren, D. Lau, and V. Sokalski, *Phys. Rev. Lett.* **119**, 027203 (2017).
- [15] L. Sánchez-Tejerina, O. Alejos, and E. Martínez, *J. Magn. Magn. Mater.* **423**, 405 (2017).
- [16] P. J. Metaxas, J. P. Jamet, A. Mougin, M. Cormier, J. Ferré, V. Baltz, B. Rodmacq, B. Dieny, and R. L. Stamps, *Phys. Rev. Lett.* **99**, 217208 (2007).
- [17] A. Hubert and R. Schäfer, *Magnetic domains: the analysis of magnetic microstructures* (Springer Science & Business Media, Berlin, 2008).
- [18] J. C. Slonczewski, *J. Appl. Phys.* **44**, 1759 (1973).
- [19] M. Li, D. Lau, M. De Graef, and V. Sokalski, *Phys. Rev. Mater.* **3**, 064409 (2019).
- [20] M. Li, A. Sapkota, A. Rai, A. Pokhrel, T. Mewes, C. Mewes, D. Xiao, M. De Graef, and V. Sokalski, *arXiv preprint arXiv:2004.07888v2* (2021).
- [21] T. Herranen and L. Laurson, *Phys. Rev. B* **96**, 144422 (2017).
- [22] Y. Yoshimura, K. J. Kim, T. Taniguchi, T. Tono, K. Ueda, R. Hiramatsu, T. Moriyama, K. Yamada, Y. Nakatani, and T. Ono, *Nat. Phys.* **12**, 157 (2016).
- [23] V. Krizakova, J. Peña Garcia, J. Vogel, N. Rougemaille, D. de Souza Chaves, S. Pizzini, and A. Thiaville, *Phys. Rev. B* **100**, 214404 (2019).
- [24] J. J. Chess, E. E. Fullerton, and B. J. McMorran, *AIP Adv.* **7**, 056807 (2017).
- [25] S. D. Pollard, J. A. Garlow, J. Yu, Z. Wang, Y. Zhu, and H. Yang, *Sci. Rep.* **8**, 14761 (2017).
- [26] J. A. Garlow, S. D. Pollard, M. Beleggia, T. Dutta, H. Yang, and Y. Zhu, *Phys. Rev. Lett.* **122**, 237201 (2019).
- [27] S. D. Pollard, J. A. Garlow, K. W. Kim, S. Cheng, K. Cai, Y. Zhu, and H. Yang, *Phys. Rev. Lett.* **125**, 272203 (2020).
- [28] J. A. Brock, M. D. Kitcher, P. Vallobra, R. Medapalli, M. P. Li, M. De Graef, G. A. Riley, H. T. Nembach, S. Mangin, V. Sokalski, and E. E. Fullerton, *Adv. Mater.*, 2101524 (2021).
- [29] J. A. Garlow, M. Beleggia, S. D. Pollard, H. Yang, and Y. Zhu, *Phys. Rev. B* **102**, 214429 (2020).